

Surface Zonal Flows Induced by Thermal Convection in Rapidly Rotating Thin Spherical Shells : A Model for Banded Structures on Jupiter and Saturn

Project Representative

Shin-ichi Takehiro Research Institute for Mathematical Sciences, Kyoto University

Authors

Shin-ichi Takehiro Research Institute for Mathematical Sciences, Kyoto University

Youhei Sasaki Department of Mathematics, Graduate School of Science, Kyoto University

Keiichi Ishioka Department of Earth and Planetary Sciences, Graduate School of Science, Kyoto University

In order to investigate the origin of the banded structures observed at the surface of Jupiter and Saturn, we perform numerical simulations of Boussinesq thermal convection in whole thin spherical shells. The Prandtl number and Rayleigh number are fixed to 0.1 and 0.05, respectively. The Ekman number and radius ratio are 10^{-4} and 0.75, or, 3×10^{-6} and 0.85, respectively. The boundary conditions at the inner and outer boundaries are free-slip and horizontally uniform temperature. We do not assume any longitudinal symmetry adopted in the previous study.

Prominent banded structures in mid- and high-latitudes cannot be found, possibly because the integration periods may be insufficient. However, eastward spike features are observed near the tangent cylinder in the surface mean zonal profiles, which is considered to be caused by angular momentum transport of topographic Rossby waves excited by the small convective motions. This mechanism may explain the origin of the strong thin jet at about 25 degrees north observed at the surface of Jupiter.

Keywords: Jupiter, Saturn, banded structure, equatorial prograde jet, Rossby waves

1. Introduction

Surface flows of Jupiter and Saturn are characterized by the broad prograde zonal jets around the equator and the narrow alternating zonal jets in mid- and high-latitudes. It is not yet clear whether those surface jets are a result of fluid motions in the “shallow” weather layer, or they are produced by convective motions in the “deep” region.

“Shallow” models consider atmospheric motions driven by the solar differential heating and the intrinsic heat flow from the deeper region under the assumption of hydrostatic balance in the vertical direction as a result of the thin atmospheric layer compared with the radius of the planet. These models can produce narrow alternating jets in mid- and high-latitudes, while the equatorial jets are not necessarily prograde.

On the other hand, “deep” models, which describe thermal convection in rapidly rotating spherical shells whose thickness is comparable to the radius of the planet, can produce equatorial prograde flows easily, while it seems to be difficult to generate alternating jets in mid- and high-latitudes.

Heimpel and Aurnou (2007) [1] proposed thin spherical shell models and show that the equatorial prograde zonal jets and alternating zonal jets in mid- and high-latitudes can be produced simultaneously when the Rayleigh number is sufficiently large and convection becomes active even inside the tangent

cylinder. However, they assumed eight-fold symmetry in the longitudinal direction and calculated fluid motion only in the one-eighth sector of the whole spherical shell. Such artificial limitation of the computational domain may influence on the structure of the global flow field. For example, zonal flows may not develop efficiently due to the insufficient upward cascade of two-dimensional turbulence, or stability of mean zonal flows may change with the domain size in the longitudinal direction.

Therefore, in the present study, we try to perform numerical simulations of thermal convection in the whole thin spherical shell domain.

2. Model

We consider Boussinesq fluid in a spherical shell rotating with a constant angular velocity Ω . The non-dimensionalized governing equations consist of equations of continuity, motion, and temperature [2]. The non-dimensional parameters appearing in the governing equations are the Prandtl number, $Pr = \nu/\kappa$, the Ekman number, $Ek = \nu/(\Omega D^2)$, and the modified Rayleigh number, $Ra = \alpha g_o \Delta T/(\Omega^2 D)$, where ν , D , κ , α , r_o , g_o , and ΔT are the kinematic viscosity, the shell thickness, the thermal diffusivity, the thermal expansion coefficient, the outer radius of the shell, the acceleration of gravity at the outer boundary, and the temperature contrast between the boundaries, respectively.

The spherical shell geometry is defined by the radius ratio, $\chi = r_i/r_o$, where r_i is the inner radius of the shell. The boundary conditions at the inner and outer boundaries are free-slip and horizontally uniform temperature.

3. Numerical method

The numerical method used in the present study is a traditional spectral method [3]. The toroidal and poloidal potentials of velocity are introduced in order to satisfy the equation of continuity. The velocity potentials and the temperature field are expanded horizontally by the spherical harmonic functions and radially by the Chebychev polynomials. The non-linear terms of the governing equations are evaluated in the physical space and are converted back into the spectral space. The time integration is performed using the Crank-Nicholson scheme for the diffusion terms and the second-order Adams-Bashforth scheme for the other terms.

4. Experimental Setup

The combinations of the non-dimensional parameters and the resolutions of the model used in this study are summarized in Table 1. The initial condition of the velocity field is state of rest and that of the temperature field is the steady conduction solution with random temperature perturbations.

In order to save computational resources, we use hyperdiffusion with the same functional form as the previous studies [1,4]: $v = v_0$ for $l \leq l_0$ while $v = v_0[1 + \epsilon(l-l_0)^2]$ for $l > l_0$, where l is total horizontal wave number.

Table 1 Summary of the nondimensional parameters and the resolutions used in this study.

| Parameters | Experiment 1 | Experiment 2 | HA2007 |
|--------------------------|----------------------------|-----------------------------|----------------------------|
| Radius ratio χ | 0.75 | 0.85 | 0.85 |
| Prandtl number Pr | 0.1 | 0.1 | 0.1 |
| Rayleigh number Ra | 0.05 | 0.05 | 0.05 |
| Ekman number Ek | 10^{-4} | 3×10^{-6} | 3×10^{-6} |
| Resolution (lon,lat,rad) | $512 \times 256 \times 65$ | $1024 \times 512 \times 65$ | $128 \times 512 \times 65$ |
| Hyper viscosity | $l_0=85, \epsilon=0.01$ | $l_0=42, \epsilon=0.01$ | ? |

5. Results

Figure 1 shows snapshots of the surface zonal flow, axial vorticity and mean zonal flow at $t=35000$ for $Ra=0.05$, $Pr=0.1$, $Ek=10^{-4}$, and $\chi=0.75$. (Experiment 1). Kinetic energy is almost saturated and the system seems to reach a statistically steady state. Obtained velocity field satisfies Taylor-Proudman theorem; it is almost uniform in the direction of the rotation axis. An equatorial prograde surface zonal jet emerges in the region outside the tangent cylinder. In the inside of the tangent cylinder, the surface zonal flows are retrograde.

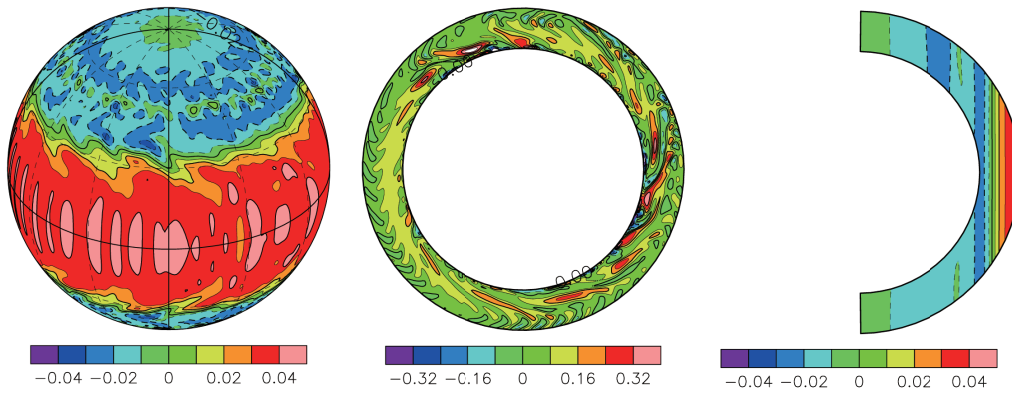


Fig. 1 Snapshots of surface zonal flow (left), axial vorticity at the equatorial cross section (center) and mean zonal flow (right) at $t=35000$ for $Ra=0.05$, $Pr=0.1$, $Ek=10^{-4}$, and $\chi=0.75$.

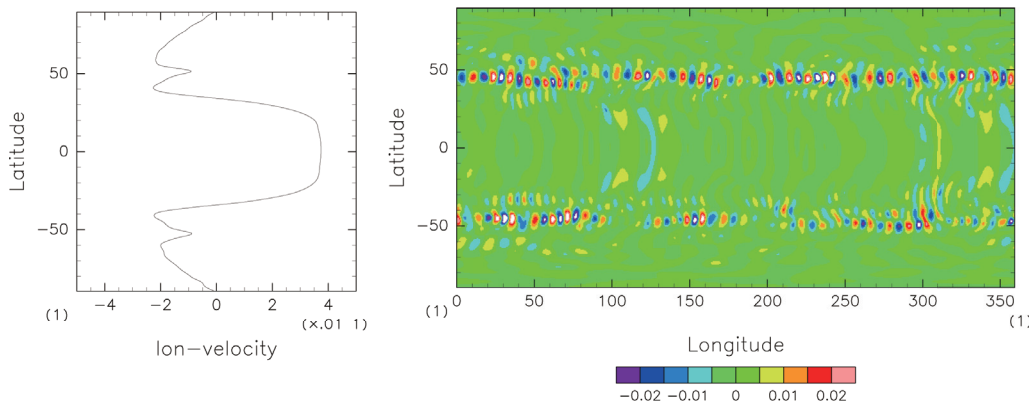


Fig. 2 Snapshots of surface mean zonal flow (left), and vertical velocity at the middle of the shell (right) at $t=35000$ for $Ra=0.05$, $Pr=0.1$, $Ek=10^{-4}$, and $\chi=0.75$.

Figure 2 shows surface mean zonal flow profile and vertical velocity at the middle of the shell for $Ra=0.05$, $Pr=0.1$, $Ek=10^{-4}$, and $\chi=0.75$. Prominent multiple banded structure cannot be found, while eastward spike features appear near the tangent cylinder in low latitudes. Correspondingly, coherent small scale convective motions exist in these latitudinal zones. It is thought that these convective motions excite topographic Rossby waves which remove westward angular momentum from these zones, producing the eastward spike features.

Figure 3 shows snapshots of the surface zonal flow, axial vorticity and mean zonal flow at $t=4700$ for $Ra=0.05$, $Pr=0.1$, $Ek=3 \times 10^{-6}$, and $\chi=0.85$ (Experiment 2). In this case, toroidal kinetic energy is still growing and the system does not reach statistically steady state. However, some characteristics of obtained velocity field are similar to those of Experiment 1. A narrower equatorial prograde surface zonal jet emerges in the region outside the tangent cylinder, while sharp retrograde zonal flows appear just inside of the tangent cylinder.

Figure 4 shows surface mean zonal flow profile and vertical velocity at the middle of the shell for $Ra=0.05$, $Pr=0.1$, $Ek=3 \times 10^{-6}$, and $\chi=0.85$. Weak multiple banded structures can be found in high latitudes, while eastward spike features appear near the tangent cylinder in low latitudes. Again, coherent small scale convective motions exist in these latitudinal zones also in this case.

6. Concluding Remark

We have tried to perform numerical simulations of thermal convection in the whole thin spherical shell domain. It cannot be found prominent banded structures in mid- and high-latitudes, however, this may be due to insufficient integration time. The eastward spike features are observed near the tangent cylinder in the surface mean zonal profiles, which is considered to be caused by the angular momentum transport of topographic Rossby waves excited by the small convective motions. This mechanism may explain the origin of the strong thin jet at about 25 degrees north observed on the surface of Jupiter.

Acknowledgement

Numerical computations were carried out on the Earth Simulator (ES2) at the Japan Agency for Marine-Earth Science and Technology.

References

[1] M. Heimpel and J. Aurnou, "Turbulent convection in rapidly rotating spherical shells: A model for equatorial and high latitude jets on Jupiter and Saturn", *Icarus*, 187, 540--557, April 2007.
 [2] U. Christensen, J. Aubert, P. Cardin, E. Dormy, S. Gibbons, G. Glatzmaier, E. Grote, Y. Honkura, C. Jones, M. Kono, M. Matsushima, A. Sakuraba, F. Takahashi, A. Tilgner, J.

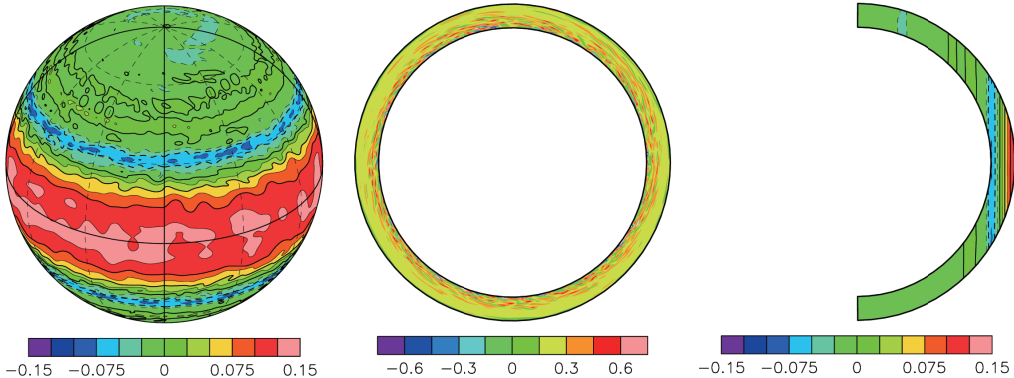


Fig. 3 Snapshots of surface zonal flow (left), axial vorticity at the equatorial cross section (center) and mean zonal flow (right) at $t=4700$ for $Ra=0.05$, $Pr=0.1$, $Ek=3 \times 10^{-6}$, and $\chi=0.85$.

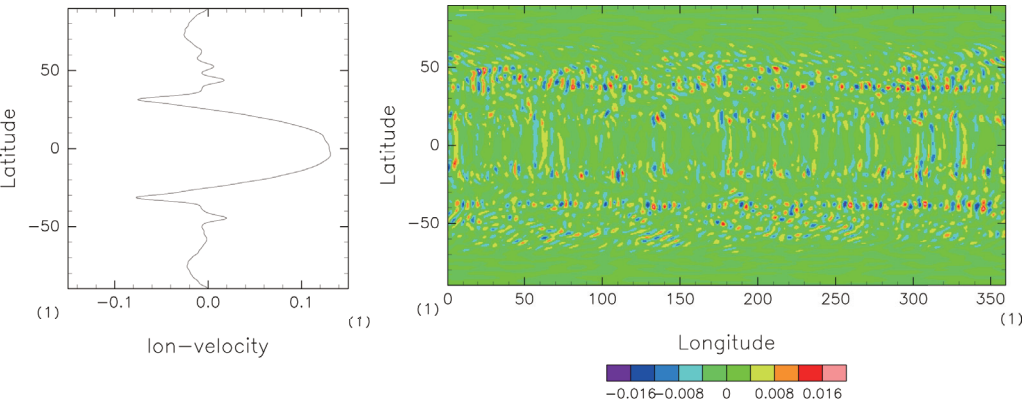


Fig. 4 Snapshots of surface mean zonal flow (left), and vertical velocity at the middle of the shell (right) at $t=4700$ for $Ra=0.05$, $Pr=0.1$, $Ek=3 \times 10^{-6}$, and $\chi=0.85$.

Wicht, and K. Zhang, "A numerical dynamo benchmark".
Physics of the Earth and Planetary Interiors 128, 25--34,
December 2001

- [3] G. A. Glatzmaier, "Numerical simulations of stellar convective dynamos. I - The model and method", Journal of Computational Physics 55, 461--484, August 1984.
- [4] W. Kuang and J. Bloxham, "Numerical Modeling of Magnetohydrodynamic Convection in a Rapidly Rotating Spherical Shell: Weak and Strong Field Dynamo Action", Journal of Computational Physics, 153, 51--81, July 1999.

高速回転する薄い球殻内の熱対流により引き起こされる表層の帯状流： 木星・土星の縞状構造のモデル

課題責任者

竹広 真一 京都大学 数理解析研究所

著者

竹広 真一 京都大学 数理解析研究所

佐々木洋平 京都大学大学院 理学研究科数学教室

石岡 圭一 京都大学大学院 理学研究科地球惑星科学専攻

木星・土星表面に観測される縞状構造の成因を探るために、薄い回転球殻ブシネスク熱対流の全球数値シミュレーションを行った。おそらく時間積分がまだ短いために、顕著な縞状構造は見出されていない。一方で、表面平均帯状流分布には東向きスパイク構造が接円筒付近外側で生成されている。これは小スケール対流により生成された地形性ロスビー波の角運動量輸送により引き起こされていると考えられる。このメカニズムは木星の北緯 25 度付近に見られる強くて細いジェットの原因を説明するかもしれない。

キーワード: 木星, 土星, 縞状構造, 赤道順行流, ロスビー波

1. はじめに

木星と土星の表層の流れは、赤道周辺の幅の広い順行ジェットと中高緯度で交互に現われる互いに逆向きの幅の狭いジェットが特徴的である。この表層のジェットが深部領域の対流によって生成されているのか、表層の流体運動の結果なのかは未だに明らかになっていない。流体層の厚さが惑星半径に比して十分小さい「浅い」モデル、すなわち、鉛直方向の静水圧近似の仮定の下で深部からの熱流と太陽加熱によって大気の運動が駆動されるモデルでは、中高緯度の交互に表われる幅の狭いジェットは再現されるものの、赤道域のジェットは必ずしも順行方向とはならない。一方で、流体層の厚さが惑星半径に匹敵する「深いモデル」、すなわち高速回転する球殻中の熱対流モデルでは、赤道域の順行するジェットは容易に生成されるものの、中高緯度の交互に表われるジェットの生成が困難である。

このような問題に対して Heimpel and Aurnou (2007) [1] は、これまでに考えられていた深いモデルよりも薄い球殻領域内の深部対流運動を考え、レイリー数が十分大きく内筒接円筒での対流が活発な場合に、赤道域の順行流と中高緯度の交互に現われる狭いジェットが共存する状態を数値的に再現した。しかしながら、彼らの研究では経度方向に 8 回対称性を仮定しており、全球の 1/8 の領域の運動しか解いていない。このような領域の制限は流れ場全体の構造に影響を与えている可能性がある。例えば、2 次元乱流的なエネルギーの upward cascade が十分に作用せず、互い違いの縞状ジェットが生成されないかもしれない。また、生成される帯状流が不安定となって縞状ジェットが壊されてしまうかもしれない。そこで本研究では、薄い球殻対流の数値計算を全球で行うことで、赤道域および中高緯度領域の帯状流が形成されるか否かを吟味した。

2. モデルと結果

モデルは回転する球殻中のブシネスク流体の方程式系で構成されている。方程式系に現われる無次元数であるプランドル数 Pr を 0.1、エクマン数 Ek を 3×10^{-6} 、球殻の内径外径比 η を 0.85、修正レイリー数 Ra を 0.05 とした。境界条件は、温度固定、応力無し条件である。初期には回転系での静止状態にランダムな温度擾乱を加えた。4700 回転まで時間積分したところ、トロイダル成分の運動エネルギーがいまだに増え続け、統計的定常状態には達していない。しかしながら、得られた流れ場の構造はテイラーブラウドマンの定理に従い回転軸方向にほぼ一様となっている (図 1 右)。表層の帯状流は、接円筒外側に相当する赤道域で一本の太い順行流が生成されている (図 1 左)。接円筒内側に相当する領域では弱い縞状構造が形成されつつあるように見える (図 2 左)。特に、接円筒に近い低緯度域で東向きスパイク状の流れ分布が観察される。球殻中層での鉛直速度分布をみると、このスパイク状の分布の緯度帯に小スケールの対流運動が規則的に存在している (図 2 右)。これらの対流運動が地形性ロスビー波を励起し、西向き角運動量を抜き去ることによってスパイク状の流れが形成されているのかもしれない。このような力学的機構は木星表面の北緯 25 度付近に見られる強くて細い西風ジェットの生成機構を示唆している可能性がある。

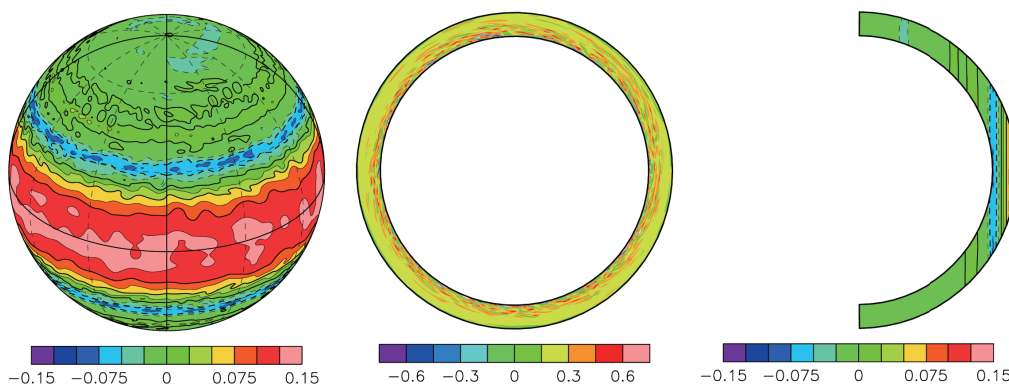


図1 表面帯状流 (左)、赤道面での回転軸方向渦度 (中央)、平均帯状流 (右) の $t=4700$ でのスナップショット。 $Ra=0.05, Pr=0.1, Ek=3 \times 10^{-6}, \eta=0.85$ の場合。

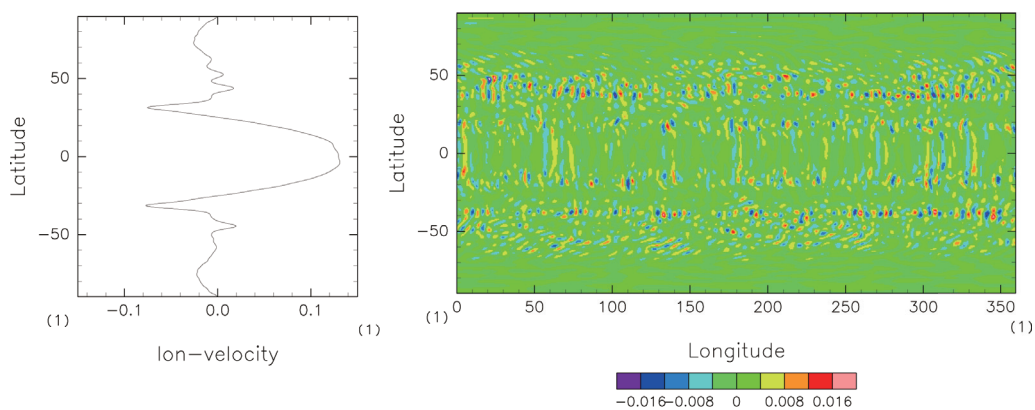


図2 表面での平均帯状流 (左) と球殻中層での鉛直速度の $t=4700$ でのスナップショット。 $Ra=0.05, Pr=0.1, Ek=3 \times 10^{-6}, \eta=0.85$ の場合。

謝辞

本研究の数値計算には海洋研究開発機構の地球シミュレータ (ES2) を用いた。

参考文献

[1] M. Heimpel and J. Aurnou, "Turbulent convection in rapidly rotating spherical shells: A model for equatorial and high latitude jets on Jupiter and Saturn", *Icarus*, 187, pp.540-557 2007.